Astron. Astrophys. 360, 463–471 (2000)

ASTRONOMY AND ASTROPHYSICS

1.4 GHz luminosity function of galaxies in the Las Campanas redshift survey and its evolution

J. Machalski and W. Godlowski

Astronomical Observatory, Jagellonian University, ul. Orla 171, 30244 Cracow, Poland (machalsk,godlowsk@oa.uj.edu.pl)

Received 22 February 2000 / Accepted 6 June 2000

Abstract. The sample of 1157 radio-identified galaxies from the Las Campanas Redshift Survey (LCRS) (Machalski & Condon 1999) is used to derive the 1.4 GHz luminosity functions of both star-forming (starburst) galaxies with the mean redshift $\langle z\rangle \approx 0.07$, and AGN-type ones with $\langle z\rangle \approx 0.18$. These functions are used as a direct measure of their evolution inferred from the evolutionary models of the entire population of radio sources. Comparing these measured functions with the corresponding local luminosity functions determined by Condon (1989) and Cotton & Condon (1998), we found that assuming the 'translation evolution' form of Condon (1984) (also Saunders et al. 1990), the amount of luminosity and/or density evolution in the LCRS sample is of the same order as the uncertainty in determination of the local functions, although the data available do not exclude mild evolution at the rate predicted by the evolutionary models. The above is supported by the starburst-type and AGN-type LCRS galaxies from the bright part of their luminosity functions which produce a spectral power density evidently higher than corresponding UGC galaxies, though the spatial densities of these UGC and LCRS galaxies are comparable. This is consistent with luminosity evolution of galaxies, at least those very luminous within their type.

Key words: surveys – galaxies: active – galaxies: evolution – radio continuum: galaxies

1. Introduction

The radio luminosity functions (hereafter RLF) of distant galaxies, directly determined in a possibly narrow redshift range, are still needed to specify the amount of cosmological evolution experienced by them, and to verify evolutionary functions mostly estimated from the observed number counts of radio sources. Usually RLFs at different frequencies were determined for radio sources in general, or for their particular types, e.g. radio-loud quasars (e.g. Petrosian 1973; Wills & Lynds 1978), radio galaxies and quasars (e.g. Windhorst 1984), or flat-spectrum and steep-spectrum sources (e.g. Peacock & Gull 1981; Dunlop & Peacock 1990). Recently, an attempt to estimate the RLF of radio sources of different morphological types, e.g. FRI and FRII (Fanaroff & Riley 1974), has been undertaken by Jackson & Wall (1999). In all these papers, the determination of RLF was based on radio-selected objects (radio sources), for which their distance and luminosity were specified, generally after optical identifications and follow-up spectroscopic measurements of their redshift.

The key characteristics, to which the amount of evolution is usually compared, is a 'local' RLF. One of the first local RLF, directly determined for nearby galaxies at 1.4 GHz by Condon (1989), was based on the radio data of optically-selected objects, namely galaxies from the Uppsala General Catalog of Galaxies (Nilson 1973, hereafter UGC). A low-luminosity extension of that function, using a cross-correlation of UGC galaxies with faint radio sources from the NRAO–VLA Sky Survey (Condon et al. 1998, hereafter NVSS), is in progress (cf. Cotton & Condon 1998). The NVSS survey is deep enough to detect radio emission from about five times more distant galaxies than those in the UGC catalogue, and thus very useful for direct determination of the RLF at redshifts beyond the local space volume around our Galaxy.

The mean redshift of radio identified UGC galaxies is only $\langle z\rangle = 0.014$. The optically-selected data, ideally suited to increase the redshift range and lookback time over which the 1.4-GHz RLF can be determined directly, come from the Las Campanas Redshift Survey of galaxies (Shectman et al. 1996, hereafter LCRS). The relevant photometric LCRS catalog contains over 90000 galaxies to limiting isophotal magnitudes of 18.2–18.5. Its photometric scale is close to R-band magnitude in the Kron–Cousins (Cousins 1976) VRI system. Spectroscopic redshifts were measured for more than 26000 galaxies fulfilling strict photometric-selection criteria (cf. Shectman et al.). Most of these redshifts are in the range $0.05 < z < 0.20$, with a mean value of about 0.10. The survey covers 0.21 sr of the sky in six elongated strips, each $1.5\deg \times 80\deg$ in size, at declinations $-3\deg, -6\deg, -12\deg, -39\deg, -42\deg$, and $-45\deg$. The area of 0.1438 sr in the first four strips is covered by the NVSS with 45″FWHM resolution to a limiting brightness of 2.5 mJy beam^{-1} at 1.4 GHz. This resolution and brightness limit are sufficient to detect radio emission from nearly all LCRS galaxies with radio luminosities $L_{1.4} \geq 10^{22.4}$ W Hz^{-1} at $z \approx 0.05$ to $L_{1.4} \geq 10^{23.6}$ W Hz^{-1} at $z \approx 0.20$. All

Send offprint requests to: J. Machalski

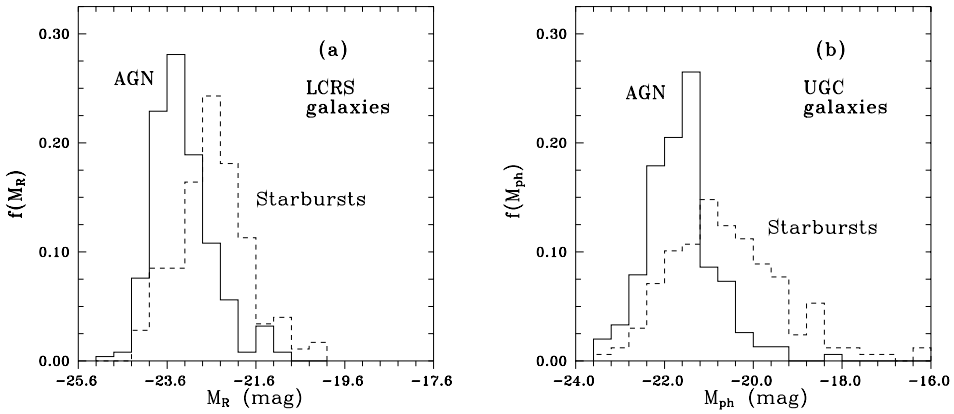

Fig. 1. a Absolute optical magnitude of LCRS galaxies powered by starburst and AGN, **b** the same for nearby UGC galaxies

calculations are performed with $H_o = 50\,\mathrm{km\,s^{-1}}$ Mpc^{-1} and $\Omega_o = 1$.

A preliminary 1.4-GHz RLF of LCRS galaxies, based on very limited radio data released up to June 1997, was communicated by Machalski & Godlowski (1998). Recently, the complete NVSS catalog and maps, the Digitized Sky Survey (DSS) images, and the IRAS Point-Source Catalog and Faint-Source Catalog (Moshir et al. 1992) have been used by Machalski & Condon (1999) to search and present the global optical, radio, and far-infrared (FIR) properties of LCRS galaxies brighter than $m_{iso} = 18.0$ mag (hereafter Paper I). Of these galaxies, 1157 have been identified with radio sources, among them 261 also identified with *IRAS* sources. The mean redshift of the radio-identified galaxies, $\langle z\rangle \approx 0.14$, is higher than the mean redshift of the optical sample, which indicates that, statistically, the radio emission was detected from galaxies with the highest optical luminosities. Paper I gives (1) details of the identification procedures and criteria, (2) criteria used to classify the principal radio energy source either as 'starburst' or 'AGN', and (3) the table containing full optical, radio, and FIR data of all 1157 galaxies, as well as examples of extended radio structures related to LCRS galaxies.

In this paper, we present the final 1.4-GHz RLF of LCRS galaxies and its comparison with the corresponding local RLF determined by Condon (1989) and Cotton & Condon (1998). Although the fraction of LCRS galaxies observed spectroscopically varied from 50 per cent to 71 per cent of those fulfilling the photometric selection criteria (cf. Lin et al. 1996), only about 35 per cent of the radio-identified galaxies have spectroscopic redshift available. Therefore, photometric redshifts of the remaining radio galaxies are estimated from their precisely measured original isophotal magnitudes and a Hubble diagram constructed from 421 identified LCRS radio galaxies with spectroscopic redshifts. The optical absolute magnitudes of these galaxies are given, and their Hubble diagram is presented in Sect. 2 along with the discussion of errors in the photometric redshift estimates. In Sect. 3, we briefly summarize the methods used to derive both the RLF [hereafter $\rho_m(L)$] and so called 'visibility' function [hereafter $\phi(L)$], very useful to interpret the observed number-counts of galaxies. An influence of the redshift errors on the space volume, and thus on the derived functions, is discussed there. Resultant $\rho_m(L)$ and $\phi(L)$ functions, determined for starburst-type and AGN-type galaxies with no account on the galaxy clustering (below), are presented in Sect. 4. In Sect. 5, these functions are compared with the corresponding local functions, and amounts of possible luminosity-evolution and density-evolution are discussed there.

2. Absolute optical magnitude and redshift estimates

2.1. Optical absolute R-band magnitude

In order to estimate redshift for the NVSS-identified galaxies which were not observed spectroscopically, we investigated the distributions of absolute optical magnitude, M_R, of about 420 LCRS radio galaxies with spectroscopic redshift, separating those powered by starbursts and AGN. These two distributions, being obviously different, are shown in Fig. 1a. Their mean values, $\langle M_R\rangle$, are -22.49 ± 0.076 mag and -23.27 ± 0.045 mag, respectively. Though these means differ significantly (the difference is 8.8 times combined error of the means), both distributions overlap to a high degree. This difference is comparable to the corresponding difference for nearby starburst-type and AGN-type UGC galaxies whose radio emission was studied by Condon & Broderick (1988) and Condon et al. (1991). The latter distributions are shown in Fig. 1b for the sake of comparison.

2.2. Redshift estimates

Because of the large overlap of the M_R–distributions for starbursts and AGN, and thus a large overlap of these galaxies on the Hubble diagrams – in order to estimate photometric redshift for other LCRS galaxies, we decided to apply a smooth increase of $\langle M_R\rangle$ with redshift rather than two different fixed values of $\langle M_R\rangle$ for starbursts and AGN. The resultant Hubble diagram for all NVSS-identified galaxies with spectroscopic redshift is shown in Fig. 2. The luminosity-distance modulus for $\Omega_o = 1$ and $\Lambda = 0$, i.e. $A(z) = 2(1 + z - \sqrt{1+z})$ is used instead of redshift (cf. Paper I). A best-fitted curve to the data points in Fig. 2 was found by minimizing the sum of squared residuals, $\Delta \log[A(z)]$, between the points and the line. Therefore, the fitted function

$$\log[A(z)] = -0.0140\, m_{\rm iso}^2 + 0.6997\, m_{\rm iso} - 8.647 \qquad (1)$$

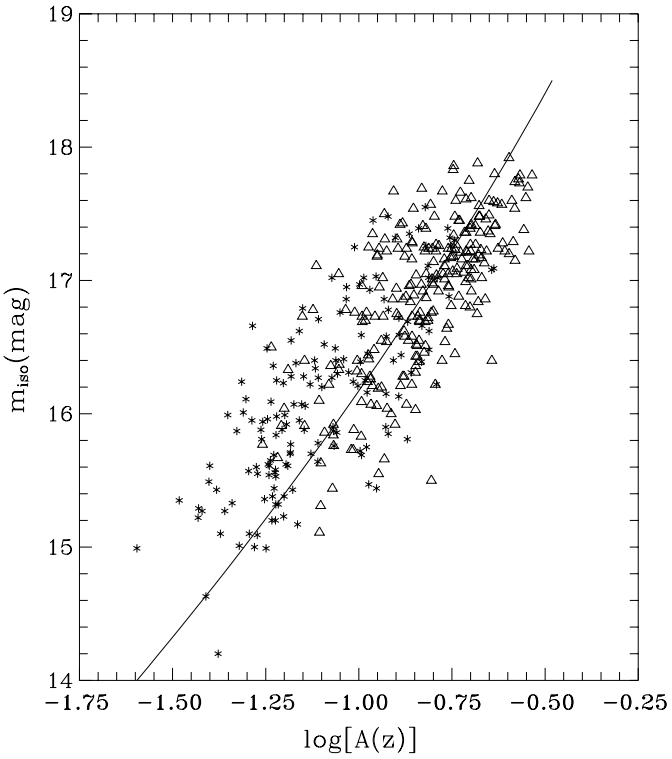

Fig. 2. Combined Hubble diagram for the radio-detected LCRS galaxies: Starbursts (asterisks), AGN (triangles). The continuous line shows the best fit to the data points

accounts for the Malmquist effect in the data: optically brighter galaxies powered by AGN dominate the LCRS sample at higher redshifts. For the sake of simplicity, Eq. (1) was numerically approximated by the form $\log z \approx -0.0114\, m_{\rm iso}^2 + 0.6182\, m_{\rm iso} - 8.016$ given in Paper I. For an easier comparison with other published Hubble diagrams (e.g. that of Eales et al. 1997), we calculate residuals, Δm, between the points and the fitted line. The distribution of these residuals is Gaussian with rms deviation $\sigma_{m_{\rm iso}} = 0.59$ mag, though the corresponding rms deviations for star-forming galaxies and AGN are even smaller, 0.45 mag and 0.41 mag respectively. These rms deviations are comparable to the corresponding deviations of 0.47 mag and 0.54 mag resulting from the K-band Hubble diagrams of 3C and 6C/B2 galaxies studied by Eales et al. [cf. their Figs. 5(a),(b)]. The spread of M_R magnitudes of all radio-identified LCRS galaxies causes an error in the redshift estimates, which in this conservative approach is

$$\sigma_z = (-0.026\, m_{\rm iso} + 0.718) z_{\rm est} \qquad (2)$$

and varies from about 0.005 to about 0.060. It corresponds to relative error ranging between $0.38 z_{\rm est}$ and $0.24 z_{\rm est}$. An influence of this error on the luminosity functions is discussed in Sect. 3.4.

3. Methods

Practically all published radio luminosity functions (RLF) were determined using the simple binned $\Sigma(1/V_{max,i})$ method of Schmidt (1968) and/or least-chi-squared fitting of their assumed parametric forms (e.g. Lynds & Wills 1972; Wall et al. 1980; Condon 1989; Dunlop & Peacock 1990). These methods are susceptible to two serious biases. First, methods using binned data usually give incorrect RLF at the lowest and highest luminosities because of non-uniform distribution of the data across the bins. Secondly, the method will be biased if density fluctuations of objects are present. For example, the optical galaxy population (at least, up to $z \lesssim 0.2$) forms spatial structures, far from uniform distribution.

The binning and clustering biases are eliminated by the 'parametric maximum likelihood' (PML) method of Sandage et al. (1979). In this method, a parametrically defined shape of the luminosity function is assumed, and the maximum likelihood solution is a set of the shape parameters for which the observed densities of objects are the most probable. However, no certain way of determining whether or not a chosen form is really the proper one is a major disadvantage of the method.

The 'stepwise maximum likelihood' (SWML) method of Efstathiou et al. (1988) is a generalization of the PML method, wherein a functional form for the luminosity function is not required. In both methods a normalization of the luminosity function is not determined, but can be found from the counts of objects (e.g. galaxies). The PML and SWML methods were used to determine the optical luminosity function of LCRS galaxies (Lin et al. 1996; Bromley et al. 1998).

The 1.4-GHz RLF of galaxies in the LCRS sample is determined using two methods: SWML and BIN. The SWML method is used to ensure a proper account for any density inhomogeneities of galaxy distribution in this sample. The general normalization of resultant Luminosity Functions for starburst-type and AGN-type galaxies is provided by the BIN method, which also allow to be directly compared with the corresponding local functions of UGC galaxies (Condon 1989). The basic aspects of both methods are shortly summarized below, and some modifications needed in the analysis of the LCRS sample are pointed out.

3.1. The SWML method

Following Condon (1989), we define $\rho_m(L)$ as the comoving space density of galaxies with radio luminosities $10^{-0.2}L$ to $10^{0.2}L$, i.e. per 'magnitude' unit $\log_m(L)$, where $\mathrm{m} = 10^{0.4}$. As in Efstathiou et al. (1988) and Saunders et al. (1990), the RLF is parametrized as N_p steps:

$$\rho_m(L) = \rho_k, \quad 10^{-0.2} L_k \le L < 10^{0.2} L_k, \quad j = 1, ..., N_p \qquad (3)$$

The maximum-likelihood solution $\{\rho_k\}$ for each k is:

$$\rho_k = n_k \left\{ \sum_{i=1}^{N} \left[f_{ik} \left(\sum_{j=1}^{N_p} f_{ij} \rho_j \right)^{-1} \right] \right\}^{-1}, \qquad (4)$$

where: N is the total number of galaxies in the sample, n_k is their number in the luminosity step, and f_{ik} ($0 \le f_{ik} \le 1$) is the fraction of the step contained in the luminosity range $[L_{\rm min}(z_i), \infty]$.

However, the radio-identified sample of LCRS galaxies is limited both by the radio and optical flux densities. The limiting fluxes are: $S_{\rm lim} = 2.5$ mJy and $F_{\rm lim} = 0.22$ mJy [corresponding to $(m_{\rm iso})_{\rm lim} = 18.0$ mag], respectively. Thus, $L_{\rm min}(z_i)$ is calculated as follows: let $L(z_i) \equiv L$ and $L_{\rm opt}(z_i) \equiv L_{\rm opt}$ be the radio and optical luminosities of ith galaxy, while $L^{(r)}_{\rm min}(S_{\rm lim}, z_i)$ and $L^{(o)}_{\rm min}(F_{\rm lim}, z_i)$ are the minimum radio and optical luminosities of a galaxy at the redshift z_i, respectively; then

$$L_{\rm min} = \left\{ \begin{array}{ll} L^{(r)}_{\rm min}, & \mathcal{R} \le \mathcal{R}_{\rm lim} \\ L^{(o)}_{\rm min}\mathcal{R}, & \mathcal{R} > \mathcal{R}_{\rm lim} \end{array} \right\}$$

where: $\mathcal{R} = L/L_{\rm opt}$, $\mathcal{R}_{\rm lim} = L^{(r)}_{\rm min}/L^{(o)}_{\rm min}$.

3.2. Visibility function

In order to compare our results with those obtained by Condon (1989) and Cotton & Condon (1998) for UGC galaxies, we calculate also the visibility function for starburst-type and AGN-type LCRS galaxies. The visibility function is the weighted luminosity function which has an advantage that it can be directly related to the normalized counts of galaxies and cosmological evolution of the RLF (cf. Condon 1989).

The function $\phi(L)$ can be calculated with the SWML method by multiplication of $\rho_m(L_i)$ times $L_i^{3/2}$ for ith galaxy, but our test calculations showed no practical difference between results obtained with the iterative algorithm and those from the relationship given by Condon (1989)

$$\log(\phi_k[{\rm Jy}^{3/2}]) \approx \log(\rho_m[{\rm mag}^{-1}{\rm Mpc}^{-3}]) + \\ + (3/2)\log(L[{\rm W\,Hz}^{-1}]) - 28.433 \qquad (5)$$

3.3. Normalization of the maximum-likelihood solutions

The RLFs derived by the SWML method are normalized by requiring that the 1.4-GHz spectral power density of galaxies with luminosities $L \ge 10^{23.6}$ W Hz^{-1} and $L \ge 10^{22.8}$ W Hz^{-1} for AGN-type and starburst-type galaxies, respectively, should be equal to that found by the BIN method. The spectral power density, defined as

$$U = \int_0^\infty L\rho(L)dL = \ln(10)\int_{-\infty}^{\infty} L^{-1/2}\phi(L)d(\log L) \qquad (6)$$

(cf. Condon 1989) has the dimension of [W Hz^{-1}Mpc^{-3}] and gives the total radio power per unit volume of space produced by the population of sources. If $d(\log L) = 0.4$, U is computed from

$$U \approx \frac{1.0857 \times 0.4}{3.40 \times 10^{-29}} \sum_{k=1}^{N_p} L_k^{-1/2}\phi_k(L). \qquad (7)$$

This procedure gives $U = 2.1 \times 10^{19}$ W Hz^{-1}Mpc^{-3} in the luminosity range from $10^{23.6}$ to $10^{25.6}$ W Hz^{-1} and $U = 3.5 \times 10^{18}$ W Hz^{-1} Mpc^{-3} in the range from $10^{22.8}$ to $10^{24.0}$ W Hz^{-1} for AGN and starbursts, respectively.

3.4. Errors of the solutions

The estimates of ρ_k and ϕ_k, derived as above, are biased by two statistical errors. The first one is the error of SWML solution which is mainly dependent on the number of objects in a bin. This error is strongly asymmetric when the numbers are small, and is calculated like that in Saunders et al. The second one arises from the redshift errors in the calculation of space volume.

In order to estimate the second error, we have performed a large number of Monte Carlo simulations in which, for each galaxy without spectroscopic redshift, an absolute magnitude was drawn by chance from the M_R distributions shown in Fig. 1a. We found that these statistical errors of ρ_k (and ϕ_k) due to erroneous redshift are also dependent on the number of galaxies in kth bin, and their values are similar to those of the SWML solutions themselves. Therefore, to calculate the statistical error of ρ_k and ϕ_k we combine both errors quadrically.

We have also checked our luminosity and visibility functions for eventual systematic errors. The fraction of spectroscopic redshift is the lowest for radio-detected LCRS galaxies with apparent magnitudes close to 18.0 mag, thus these galaxies may introduce a systematic error into ρ_k. However, they are mostly identified as the AGN-type (cf. Machalski & Condon). Assuming that their M_R magnitudes do not differ significantly from corresponding magnitudes of 3C and 6C radio galaxies, one can see that the redshift estimate of a LCRS galaxy with $m_{\rm iso} \approx 18.0$ mag, computed from Eq. (1), is compatible with that from Rmag – redshift relation given by Eales (1985). Therefore, we claim that systematic errors in our results are rather unlikely.

4. 1.4 GHz luminosity and visibility functions

The resulting estimates of the $\rho_m(L, z_s)$ and $\phi(L, z_s)$ functions for starburst-type and AGN-type LCRS galaxies, computed from Eqs. (4) and (5) and normalized using the prescriptions given in Sect. 3.3, are tabulated in Tables 1 and 2. The rms errors of these estimates are computed as described in Sect. 3.4.

A number of parametric forms for luminosity functions were fitted to these estimates. As a result, we found that Schechter's function is not satisfactory, as it is too narrow for radio-identified galaxies. Likewise descriptions using single power-law, as well as the Gaussian form proposed by Sandage et al. (1985), are not suitable. The best fit either to starbursts or AGN galaxies has been achieved by the function given by Saunders et al.

$$\rho_m(L) = C\left(\frac{L}{L_*}\right)^{1-\alpha} \exp\left\{-\frac{1}{2}\left[\frac{\log(1+L/L_*)}{\sigma}\right]^2\right\}, \qquad (8)$$

which behaves as a power-law for $L \ll L_*$ and as a Gaussian in $\log L$ for $L \gg L_*$. Besides, its logarithmic form, transformed to the logarithm of visibility function $\log\phi(L)$ by Eq. (5) is almost identical, within the luminosity range involved, with the parabolic form

$$\log\phi(L) = Y - \left[\frac{\log L - X}{W}\right]^2 \qquad (9)$$

Table 1. 1.4 GHz luminosity functions based on LCRS galaxies

		ALL		STARBURSTS		AGN
$\log L_{1.4}$	N	$\log \rho_m$	N	$\log \rho_m$	N	$\log \rho_m$
(W Hz^{-1})		(mag^{-1}Mpc^{-3})		(mag^{-1}Mpc^{-3})		(mag^{-1}Mpc^{-3})
20.2	1	$-2.82^{+0.83}_{-0.97}$	1	$-2.82^{+0.83}_{-0.97}$		
20.6	0	< -2.88	0	< -2.88		
21.0	5	$-3.18^{+0.25}_{-0.40}$	5	$-3.18^{+0.25}_{-0.40}$		
21.4	3	$-3.73^{+0.31}_{-0.48}$	3	$-3.73^{+0.31}_{-0.48}$		
21.8	25	$-3.49^{+0.13}_{-0.15}$	25	$-3.49^{+0.13}_{-0.15}$		
22.2	68	$-3.66^{+0.09}_{-0.10}$	68	$-3.66^{+0.09}_{-0.10}$		
22.6	120	$-4.13^{+0.07}_{-0.08}$	119	$-4.13^{+0.07}_{-0.08}$	1	$-6.40^{+0.83}_{-0.97}$
23.0	151	$-4.65^{+0.06}_{-0.07}$	138	$-4.68^{+0.07}_{-0.07}$	13	$-5.84^{+0.15}_{-0.18}$
23.4	182	$-5.17^{+0.05}_{-0.06}$	112	$-5.38^{+0.08}_{-0.09}$	70	$-5.58^{+0.08}_{-0.08}$
23.8	223	$-5.48^{+0.05}_{-0.05}$	27	$-6.53^{+0.13}_{-0.16}$	196	$-5.52^{+0.05}_{-0.05}$
24.2	169	$-5.73^{+0.05}_{-0.06}$	4	$-7.43^{+0.26}_{-0.37}$	165	$-5.74^{+0.05}_{-0.06}$
24.6	120	$-5.87^{+0.06}_{-0.07}$	0	< -7.72	120	$-5.87^{+0.06}_{-0.07}$
25.0	62	$-6.16^{+0.08}_{-0.09}$			62	$-6.16^{+0.08}_{-0.09}$
25.4	18	$-6.70^{+0.13}_{-0.15}$			18	$-6.70^{+0.13}_{-0.15}$
25.8	9	$-7.00^{+0.17}_{-0.21}$			9	$-7.00^{+0.17}_{-0.21}$
26.2	1	$-7.95^{+0.83}_{-0.97}$			1	$-7.95^{+0.83}_{-0.97}$
26.6	0	< -8.04				
Total	1157		502		655	

Table 2. 1.4 GHz visibility functions based on LCRS galaxies

		ALL		STARBURSTS		AGN
$\log L_{1.4}$	N	$\log \Phi$	N	$\log \Phi$	N	$\log \Phi$
(W Hz^{-1})		(Jy$^{3/2}$)		(Jy$^{3/2}$)		(Jy$^{3/2}$)
20.2	1	$-0.96^{+0.83}_{-0.97}$	1	$-0.96^{+0.83}_{-0.97}$		
20.6	0	< -0.51	0	< -0.51		
21.0	5	$-0.11^{+0.25}_{-0.40}$	5	$-0.11^{+0.25}_{-0.40}$		
21.4	3	$-0.06^{+0.31}_{-0.48}$	3	$-0.06^{+0.31}_{-0.48}$		
21.8	25	$+0.78^{+0.13}_{-0.15}$	25	$+0.78^{+0.13}_{-0.15}$		
22.2	68	$+1.21^{+0.09}_{-0.10}$	68	$+1.21^{+0.09}_{-0.10}$		
22.6	120	$+1.34^{+0.07}_{-0.08}$	119	$+1.34^{+0.07}_{-0.08}$	1	$-0.93^{+0.83}_{-0.97}$
23.0	151	$+1.42^{+0.06}_{-0.07}$	138	$+1.39^{+0.07}_{-0.07}$	13	$+0.23^{+0.15}_{-0.18}$
23.4	182	$+1.50^{+0.05}_{-0.06}$	112	$+1.28^{+0.08}_{-0.09}$	70	$+1.09^{+0.08}_{-0.08}$
23.8	223	$+1.79^{+0.05}_{-0.05}$	27	$+0.74^{+0.13}_{-0.16}$	196	$+1.74^{+0.05}_{-0.05}$
24.2	169	$+2.14^{+0.05}_{-0.06}$	4	$+0.44^{+0.26}_{-0.37}$	165	$+2.13^{+0.05}_{-0.06}$
24.6	120	$+2.59^{+0.06}_{-0.07}$	0		120	$+2.59^{+0.06}_{-0.07}$
25.0	62	$+2.91^{+0.08}_{-0.09}$			62	$+2.91^{+0.08}_{-0.09}$
25.4	18	$+2.97^{+0.13}_{-0.15}$			18	$+2.97^{+0.13}_{-0.15}$
25.8	9	$+3.27^{+0.17}_{-0.21}$			9	$+3.27^{+0.17}_{-0.21}$
26.2	1	$+2.91^{+0.83}_{-0.97}$			1	$+2.91^{+0.83}_{-0.97}$
Total	1157		502		655	

In order to compare the RLF for LCRS galaxies with the local functions directly determined for UGC galaxies by Condon (1989) and Cotton & Condon (1998), we also fit the hyperbolic form

$$\log \phi(L) = Y - \left\{ B^2 + \left[\frac{\log L - X}{W} \right]^2 \right\}^{1/2} \qquad (10)$$

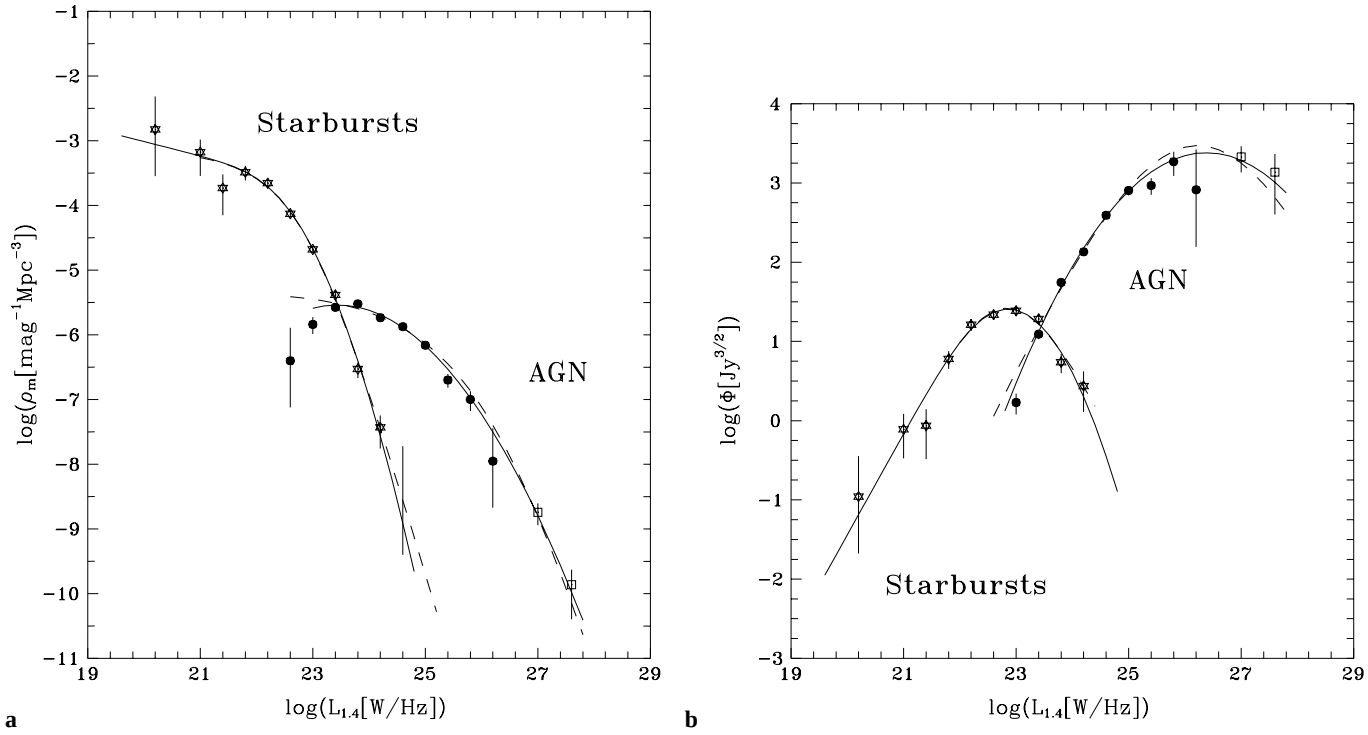

Fig. 3. a 1.4 GHz luminosity function of LCRS galaxies: Starbursts (stars), AGN (filled circles); **b** corresponding visibility functions. Their parametric representations by the Saunders' and hyperbolic functions are marked by the solid and dashed curves, respectively

Table 3. Parametric solutions for starburst-type and AGN-type LCRS galaxies

Function	Parameter[dimension]	STARBURSTS	AGN
Saunders et al.	$\log(L_*[\mathrm{W\,Hz^{-1}}])$	21.73 ± 0.37	23.77 ± 1.03
	α	1.22 ± 0.27	1.24 ± 0.38
	σ	0.61 ± 0.05	0.95 ± 0.08
	$\log(C[\mathrm{mag^{-1}Mpc^{-3}}])$	-3.40 ± 0.17	-5.51 ± 0.30
	χ^2	0.77	0.82
parabola	$X[\mathrm{W\,Hz^{-1}}]$	22.83 ± 0.05	26.50 ± 0.18
	W	1.36 ± 0.07	2.11 ± 0.12
	$Y[\mathrm{mag^{-1}Mpc^{-3}}]$	1.40 ± 0.03	3.37 ± 0.08
	χ^2	0.90	0.79
hyperbola	$X[\mathrm{W\,Hz^{-1}}]$	22.84 ± 0.05	26.39 ± 0.16
	B	1.78 ± 1.14	3.23 ± 0.45
	W	0.64 ± 0.24	0.70 ± 0.35
	$Y[\mathrm{mag^{-1}Mpc^{-3}}]$	3.20 ± 1.74	6.65 ± 0.46
	χ^2	0.87	0.96

to our $\log \phi(L)$ estimates. The best-fitted parameters of the Saunders', parabolic, and hyperbolic functions are given in Table 3. The errors quoted in Table 3 are 1σ uncertainty for particular parameter when all others are optimized for maximum likelihood. The non-parametric estimates of the $\rho_m(L, z_s)$ and $\phi(L, z_s)$ functions, and their parametric representations are plotted in Figs. 3a and 3b, respectively. The function estimates for starbursts are shown by the star symbol, while those for AGN – by filled circles.

The sky area surveyed by the LCRS is 0.14 sr only, thus the space volume involved is insufficient for a proper determination of the RLF at its bright ends. To determine this for the AGN subsample, we selected all powerful radio galaxies, lying on 4.1 sr of the northern sky and fulfilling the LCRS selection criteria, i.e. with $z \leq 0.27$ and $R < 17.75$ mag, and used them to extend the $\rho_m(L)$ and $\phi(L)$ functions for AGN to 1.4 GHz luminosity of about $10^{27.6}$ W Hz^{-1}. The estimates of relevant luminosity- and visibility-function derived from these data are plotted in Figs. 3a and 3b with open squares. Vertical bars indicate the statistical error of each estimate, quoted in Table 2 and 3. The solid curves denote the best fit to Saunders' function, while the dashed curves – the equivalent hyperbolic representation.

5. Comparison with the local 1.4 GHz RLF and the evolution

In the previous sections we did not account for possible effects of evolution that might be present in the LCRS sample. No significant amount of evolution can be expected in this sample because redshifts of the most luminous LCRS galaxies do not exceed 0.27. Nevertheless, it is tempting to compare the RLF for LCRS galaxies to the local RLFs based on UGC galaxies. The only 1.4 GHz luminosity functions of galaxies determined *directly* are those by Condon (1989) and Cotton & Condon (1998). The corresponding parametric forms of the two local functions (given in the original papers) are referred here to as LLF(89) and LLF(98), respectively. The latter one, however, is rather preliminary (W.D. Cotton, private communication).

To quantify the evolution, we follow Condon (1984), Saunders et al. (1990) and others, assuming that the RLF evolves without changing its shape according to

$$\rho_m(L,z) = g(z)\,\rho_m[L/f(z), z \approx 0], \tag{11}$$

where $g(z)$ and $f(z)$ represent evolutions of density and luminosity, respectively. These two evolutionary functions can be found by fitting the local function (in its logarithmic form) to the $\log[\rho_m(L,z)]$ with some horizontal and vertical shifts

$$\log[\rho_m(\log L, z)] = \log[\rho_m(\log L - \Delta X)] + \Delta Y$$

The fitted horizontal shift in the $\log(L)$ axis, ΔX, corresponds to $\log(f_s)$, while a vertical shift in the $\log(\rho_m)$ axis, ΔY, corresponds to $\log(g_s)$. Here the suffix s stands for the sample. The fitting procedure by the χ^2 method revealed that the formal best-fit solutions are not always reliable in the case of the UGC and LCRS samples. In Fig. 4, we compare the luminosity functions for starburst-type and AGN-type LCRS galaxies, parametrized using Saunders' and hyperbolic forms with their parameters given in Table 3, to the local luminosity functions for UGC galaxies represented by the models LLF(89) and LLF(98). Saunders' forms are indicated by the solid curves, while the hyperbolic forms – by the long-dash curves. The local functions are marked by short-dash curves and asterisks for the LLF(89) and LLF(98) models, respectively.

The plots in Fig. 4 show that the local 1.4 GHz RLF is inconclusive. Evidently, the extention of radio detections of UGC galaxies to the NVSS flux-density limit of 2.5 mJy, has resulted in an expansion of the low-luminosity range of the LLF. Matching these two local functions between themselves, the formal best-fit solutions are: $\Delta X = +0.16 \pm 0.03$, $\Delta Y = -0.19 \pm 0.04$ for starbursts, and $\Delta X = +0.31 \pm 0.08$, $\Delta Y = -0.10 \pm 0.10$ for AGN galaxies. Hence we conclude that the actual error in ΔX and/or ΔY is about 0.2–0.3, and any displacement (i.e. luminosity or density evolution function) less than $3 \times 10^{0.2}$ – $3 \times 10^{0.3}$ remains uncertain in view of the statistics provided by the UGC data. Therefore, in order to compare the RLFs of LCRS galaxies to a LLF, we averaged the LLF(89) and LLF(98) functional forms, and then fitted these averaged functions of UGC starbursts and AGN to the RLF estimates of the corresponding LCRS galaxies with ΔX and ΔY shifts.

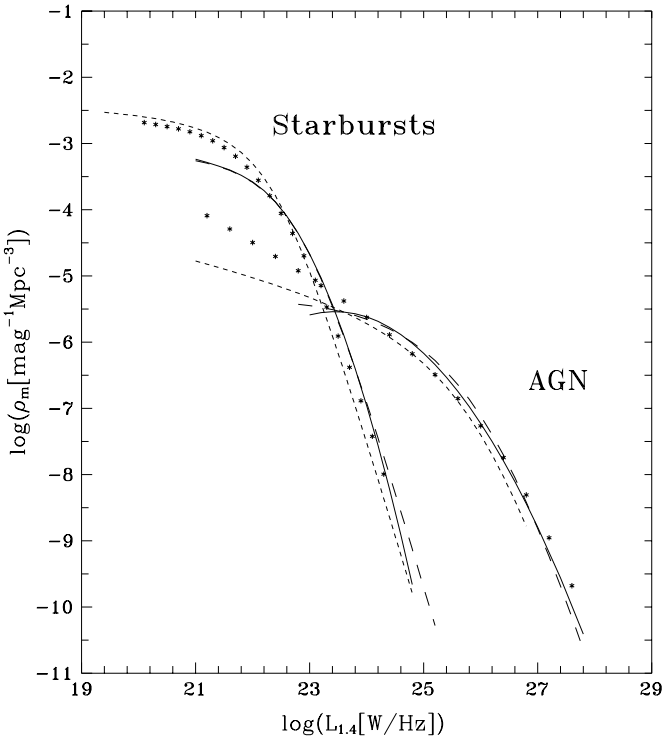

Fig. 4. Comparison of the 1.4 GHz luminosity functions of LCRS galaxies with the corresponding local functions based on UGC galaxies. Saunders' and hyperbolic functions for LCRS galaxies are shown by the solid and long-dash curves, respectively; the original hyperbolic functions for UGC galaxies are indicated by short-dash curves (LLF89 model) and asterisks (LLF98 model)(cf. the text)

In effect, $\Delta X = 0.21 \pm 0.06$; $\Delta Y = -0.23 \pm 0.09$ and $\Delta X = 0.12 \pm 0.12$; $\Delta Y = 0.02 \pm 0.08$ were found for the starburst-type and AGN-type galaxies. The quoted formal errors of the above shifts are rms errors in the χ^2 fitting method. The actual errors of these shifts are greater than the values $\log f \approx 0.16$ and $\log g \approx 0.06$, expected from the evolutionary model of Condon (1984) at $z \approx 0.14$. Thus, we have to conclude that LCRS galaxies do not show any detectable cosmological evolution in the form described by Eq. 11. A similar conclusion was recently drawn by Mobasher et al. (1999) on the basis of 1.4-GHz luminosity functions of faint star forming and elliptical galaxies with mean redshift of about 0.3, detected during the Phoenix Deep Survey (Hopkins et al. 1998).

However, it should be emphasized that the above conclusions about the absence of significant cosmological evolution in the redshift range $0 < z < 0.3$ have resulted from the analysis of RLFs of the local (UGC) and more distant (LCRS) galaxies, under assumption that the shape of these functions does not change. In other words, the same evolution, either luminosity or density, was assumed for a given type of galaxies (cf. Eq. 11), in spite of their radio luminosity. Some indications that this may not be the case come from a comparison of the spectral power density (defined in Sect. 3.3) and the radial density of UGC and LCRS galaxies *limited* to their highest luminosities, fulfilling $L \geq L_{min}$, where L_{min} is the minimal luminosity of a galaxy

Table 4. 1.4 GHz spectral power density and radial density of starburst-type galaxies with $L_{1.4} \geq 10^{22.8}$[W Hz^{-1}], and AGN-type galaxies with $L_{1.4} \geq 10^{24.0}$[W Hz^{-1}]

Sample		UGC	LCRS
Starburst	Redshift range	$z < 0.01$	$0.01 \leq z < 0.075$
galaxies	Sky area a[sr]	4.87	0.1438
	Volume $V[10^6\mathrm{Mpc}^3]$	0.343	3.710
	No. galaxies$[N \pm \sqrt{N-2}]$	4 ± 1.4	53 ± 7.1
	U$[10^{18}$W Hz^{-1}Mpc$^{-3}]$	0.87 ± 0.44	1.67 ± 0.32
	U(LCRS)/U(UGC)	1	1.92 ± 0.60
	ϱ(LCRS)/ϱ(UGC)	1	1.23 ± 0.27
AGN	Redshift range	$z < 0.04$	$0.04 \leq z < 0.26$
galaxies	Sky area a[sr]	4.87	0.1438
	Volume $V[10^7\mathrm{Mpc}^3]$	2.055	10.704
	No. galaxies $[N \pm \sqrt{N-2}]$	58 ± 7.8	354 ± 18.8
	U$[10^{19}$W Hz^{-1}Mpc$^{-3}]$	1.93 ± 0.65	2.92 ± 0.61
	U(LCRS)/U(UGC)	1	1.51 ± 0.19
	ϱ(LCRS)/ϱ(UGC)	1	1.17 ± 0.12

attained with the flux-density limit of a given sample at the redshift z. If a chosen z is close to the highest redshifts in this sample, the Malmquist bias in it is completely eliminated. The radial density is determined in a broad range of luminosities as

$$\varrho = \frac{N}{V} = \frac{N}{(a/4\pi)V(z)}, \tag{12}$$

where N is the number of galaxies in a sample with $L \geq L_{\min}$, a[sr] is the sky area of the survey, and $V(z)$[Mpc^3] – space volume within the redshift z.

In Table 4, the spectral power density and radial density of starburst galaxies with $L_{1.4} \geq 10^{22.8}$ W Hz^{-1} and AGN-type galaxies with $L_{1.4} \geq 10^{24.0}$ W Hz^{-1} in the UGC and LCRS samples are compared. These limiting luminosities are chosen to assure that all starbursts with 1.4 GHz luminosity above $10^{22.8}$ W Hz^{-1} in the UGC and LCRS samples could be detected up to the redshift of 0.01 and 0.075, respectively, as well as AGN galaxies more luminous than $10^{24.0}$ W Hz^{-1} – up to the redshift of 0.04 and 0.26, respectively. The last two lines in Table 5 indicate that both starburst-type and AGN-type galaxies from the brighter part of their luminosity functions show a discrepancy between the variations of spectral power density and radial density of nearby (UGC) and distant (LCRS) galaxies. While the radial densities (within the broad luminosity range) are statistically comparable, the spectral power density for both types of LCRS galaxies is evidently higher than those for corresponding UGC galaxies. Although a statistical significance of the differences in spectral density is not too high, its increase of about 50%, relative to the local value for AGN, corresponds to the expected luminosity evolution of order $f(z) \sim (1+z)^{3\pm1}$, i.e. $(1+0.18)^{3\pm1} = 1.64$ for $\langle z \rangle \simeq 0.18$ for LCRS AGN galaxies.

An intriguing fluctuation can be seen if 354 AGN galaxies in Table 4 are divided into two redshift ranges: $0.04 \leq z < 0.18$ and $0.18 \leq z < 0.26$. In this case the U(LCRS)/U(UGC) ratios equal to 0.87 ± 0.06 and 1.62 ± 0.05, respectively, while ϱ(LCRS)/ϱ(UGC) ratios equal to 1.25 ± 0.07 and 1.12 ± 0.08. The data, available here, are not sufficient to specify whether this effect reflects some real clustering of radio galaxies or is only a statistical fluctuation of their spatial density. The radial density and clustering of radio galaxies in the LCRS sample will be analysed in a separate paper (in preparation).

6. Conclusions

The 1.4 GHz luminosity functions of star-forming (starburst) and AGN galaxies in the LCRS sample (Paper I) are well described by Saunders' functional form, though the hyperbolic form of the weighted luminosity function, i.e. visibility function (cf. Condon 1984) is equally acceptable.

Their evolution in the 'translation' form, given by Eq. (11), is uncertain at redshifts characteristic for the LCRS sample: $\langle z \rangle \simeq 0.07$ for starbursts and $\langle z \rangle \simeq 0.18$ for AGN. This is because an amount of luminosity and/or density evolution inferred from the evolutionary models is of the same order as uncertainties of the local luminosity functions determined from UGC galaxies (Condon 1989; Cotton & Condon 1998). However, the direct comparison of the spectral power density and radial density of UGC and LCRS starburst and AGN galaxies with 1.4 GHz luminosities exceeding $10^{22.8}$W Hz^{-1} and $10^{24.0}$W Hz^{-1}, respectively (i.e. galaxies from the brighter part of their luminosity functions) agree with a luminosity evolution $f(z) \propto (1+z)^{3\pm1}$.

Acknowledgements. Authors acknowledge the support from the State Committee for Scientific Research (KBN) under contract PB 0266/PO3/99/17.

References

Bromley B.C., Press W.H., Lin H., Kirshner R.P., 1998, ApJ 505, 25
Condon J.J., 1984, ApJ 287, 461
Condon J.J., 1989, ApJ 338, 13
Condon J.J., Broderick J.J., 1988, AJ 96, 30
Condon J.J., Frayer B.T., Broderick J.J., 1991, AJ 101, 362
Condon J.J., Cotton W.D., Greisen E.W., et al., 1998, AJ 115, 1693 (NVSS)

Cotton W.D., Condon J.J., 1998, In: Bremer M.N., Jackson N., Perez-Fournon I. (eds.) Observational Cosmology with the New Radio Surveys. Kluwer, Dordrecht, p. 45
Cousins A.W.J., 1976, Mem. R. Astron. Soc. 81, 25
Dunlop J.S., Peacock J.A., 1990, MNRAS 247, 19
Eales S.A., 1985, MNRAS 217, 179
Eales S., Rawlings S., Law-Green D., Cotter G., Lacy M., 1997, MNRAS 291, 593
Efstathiou G., Ellis R.S., Peterson B.A., 1988, MNRAS 232, 431
Fanaroff B.L., Riley J.M., 1974, MNRAS 167, 31P
Hopkins A.M., Mobasher B., Cram L., Rowan-Robinson M., 1998, MNRAS 296, 839
Jackson C.A., Wall J.V., 1999, MNRAS 304, 160
Lin H., Kirschner R.P., Shectman S.A., et al., 1996, ApJ 464, 60
Lynds R., Wills D., 1972, ApJ 172, 531
Machalski J., Condon J.J., 1999, ApJS 123, 41 (Paper I)
Machalski J., Godlowski W., 1998, In: Bremer M.N., Jackson N., Perez-Fournon I. (eds.) Observational Cosmology with the New Radio Surveys. Kluwer, Dordrecht, p. 51
Mobasher B., Cram L., Georgakakis A., Hopkins A., 1999, MNRAS 308, 45
Moshir M., Kopan G., Conrow T., et al., 1992, Explanatory Supplement to the IRAS Faint Source Survey, Version 2, JPL D-10015 8/92 (Jet Propulsion Laboratory, Pasadena)
Nilson P., 1973, Uppsala General Catalogue of Galaxies (Uppsala Astronomical Observatory) (UGC)
Peacock J.A., Gull S.F., 1981, MNRAS 196, 611
Petrosian V., 1973, ApJ 183, 359
Sandage A., Tammann G.A., Yahil A., 1979, ApJ 232, 352
Sandage A., Binggeli B., Tammann G.A., 1985, AJ 90, 1759
Saunders W., Rowan-Robinson M., Lawrence A., et al., 1990, MNRAS 242, 318
Shectman S.A., Landy S.D., Oemler A., et al., 1996, ApJ 470, 172
Schmidt M., 1968, ApJ 151, 393
Wall J.V., Pearson T.J., Longair M.S., 1980, MNRAS 193, 683
Wills D., Lynds R., 1978, ApJS 36, 317
Windhorst R.A., 1984, Ph.D. Thesis (Sterrewacht Leiden)